Comparative Evaluation of Low-Cost LiDAR and Ultrasonic Sensors for River Level Monitoring

Klaus Dieter Kupper[1], **Jordan Passinato Sausen**[1], **Mauricio de Campos**[1]

[1]Universidade do Vale do Itajaí (UNIVALI) – Itajaí, SC – Brazil

klausdk1999@gmail.com, jordan.sausen@univali.br, mauricio.campos@univali.br

Abstract. *Flood monitoring in data-scarce tributaries remains limited by the high cost of conventional hydrometric infrastructure. This paper presents a comparative evaluation of three low-cost non-contact sensors, two LiDAR and one ultrasonic, for river level measurement, validated through controlled laboratory tests and real-world bridge deployments under contrasting weather conditions. Results reveal three key findings: (1) direct solar radiation reduces LiDAR availability by up to 67%, with severity depending on sensor design; (2) wide-angle line-beam optics provide up to 8× improvement in measurement stability over dynamic water surfaces compared to narrow spot-beam configurations; and (3) water turbidity confirms improved LiDAR accuracy. ISO 4373:2022 benchmarking shows that the ultrasonic sensor achieves consistent availability across conditions, while LiDAR sensors require careful design-level selection based on deployment environment.*

1. Introduction

Floods account for the largest share of natural disaster fatalities and economic losses worldwide, since the 1970s, 44% of all recorded disaster events have been flood-related [Jonkman 2005, Pörtner et al. 2022]. A warmer atmosphere holds approximately 7% more moisture for every 1°C of warming [Pörtner et al. 2022], intensifying extreme precipitation events. In regions such as Brazil's Vale do Itajaí, recurrent flooding has caused significant socioeconomic impacts [Santos et al. 2014], a situation expected to worsen under climate change projections. The catastrophic 2024 floods in Rio Grande do Sul, where human-induced climate change made the extreme rainfall event twice as likely [Otto et al. 2024], further underscore the urgency of improved monitoring infrastructure.

These trends align with UN SDG 11 and SDG 13 [United Nations General Assembly 2015] and the Sendai Framework [United Nations Office for Disaster Risk Reduction 2015], which emphasize expanding early warning systems in vulnerable regions. However, conventional hydrometric stations rely on expensive equipment, limiting deployment to major waterways while data-scarce tributaries remain unmonitored [Borga et al. 2014]. The convergence of low-cost sensors, IoT microcontrollers, and LoRaWAN communication [Sun et al. 2022] enables affordable monitoring nodes for these gaps [Kabi et al. 2023, Tawalbeh et al. 2023].

Two aspects of low-cost LiDAR behavior over water remain unquantified. First, although ambient sunlight is a recognized noise source in LiDAR, no published work measures its effect over water, where reflectivity is inherently low, creating marginal signal-to-noise conditions. Second, all existing LiDAR water-monitoring studies employ narrow spot-beam sensors; none evaluates how wide line-beam geometry affects measurement

stability over dynamic surfaces. More broadly, the literature lacks a side-by-side comparison of ultrasonic and LiDAR sensors under identical environmental stressors within a complete lab-to-field validation pipeline.

This paper addresses these gaps through a Lab-to-Bridge evaluation of three low-cost sensors (two LiDAR, one ultrasonic), first characterized under controlled environmental stressors, then deployed on a river under rainy and sunny conditions. The main contributions are: (1) identification of solar radiation as a critical, sensor-design-dependent LiDAR limitation for water level monitoring; (2) characterization of beam geometry (line-beam vs. spot-beam) as a sensor selection criterion; and (3) ISO 4373:2022 compliance benchmarking under field conditions.

2. Related Work

Recent reviews have consolidated advances in sensing, communication, and AI-enabled systems for environmental monitoring [Kupper et al. 2025, Wu et al. 2023, Mohindru 2023]. Among low-cost non-contact options, ultrasonic sensors are the most widely adopted, with evaluations reporting mean errors below 2% at distances up to 4 m [Pereira et al. 2022], sub-millimeter resolution [Mohammed et al. 2019], and sub-centimeter temperature-compensated accuracy [MasoudiMoghaddam et al. 2024]. However, ultrasonic sensors are limited by range ($\leq$5 m), temperature sensitivity, and wind susceptibility [Tarulescu and Tarulescu 2014].

LiDAR-based water level measurement is less explored. Terrestrial LiDAR presents challenges with specular reflection on clear water [Paul et al. 2020], though inclined installations have shown promise for flash flood detection [Tamari and Guerrero-Meza 2016] and near-infrared LiDAR requires a minimum turbidity of $\sim$700 NTU for reliable detection [Jannata et al. 2021]. Several LoRa-based flood monitoring systems have been validated, including 18-month deployments [Kabi et al. 2023], autonomous solar-harvesting monitors [Ragnoli et al. 2020], and beat-frequency sensors achieving millimeter accuracy [DAO et al. 2025].

Despite these advances, no prior work has systematically compared LiDAR and ultrasonic sensors under contrasting environmental conditions for river monitoring, nor has beam geometry been considered as a selection criterion.

3. Materials and Methods

Five non-contact sensors were initially considered. After preliminary testing, two were eliminated: the TF-Luna LiDAR was excluded because its maximum range of 7 m is insufficient for typical bridge-to-river distances and it shares the same optical design as the TF02-Pro, making it redundant; the HC-SR04 ultrasonic sensor was excluded due to its lack of environmental sealing and low range, which makes it unsuitable for outdoor deployment under rain and humidity. The remaining three sensors advanced to full evaluation (Table 1).

A three-phase Lab-to-Bridge approach was adopted (Table 2), designed to progressively increase environmental complexity while isolating specific variables that affect sensor performance.

In Phase 1, sensors were evaluated for distance accuracy (5–25 m against a solid wall, reference distances measured with tape measure), rain interference (simulated heavy

Table 1. Sensors selected for comparative evaluation.

Sensor	Type	Range	Beam	Sunlight
TF02-Pro	LiDAR	0.1–40 m	3° spot	100 kLux
TF-Nova	LiDAR	0.1–14 m	$14° \times 1°$ line	Not rated
JSN-SR04T	Ultrasonic	0.23–6 m	Conical	Immune

Table 2. Summary of the three-phase evaluation methodology.

Phase	Objective	Tests	Outputs
1	Controlled environment	Distance range, rain interference, water surface	Sensor limits, baseline accuracy
2	Bridge validation	Point measurements at 4.1 m and 5.4 m	Field accuracy, beam geometry
3	Extended field deployment	Multi-hour rainy and sunny operation	ISO 4373 class, env. sensitivity

rainfall), and water surface detection (1–3 m over clear and turbid water). Phase 2 consisted of point measurements at two bridges over a river under overcast conditions. Phase 3 comprised two multi-hour deployments at the same bridge ($\sim$3.1 m sensor-to-water) under contrasting weather: overcast/rainy (Feb 7, 2026; 5 hours; 11 mm rainfall) and clear sky/sunny (Feb 8, 2026; 3.5 hours). Two LoRaWAN sensor nodes transmitted readings every 1–2 minutes.

Each wake cycle acquires a burst of 10 distance readings, applies median filtering, and performs temperature compensation for ultrasonic measurements. An adaptive transmission strategy (Table 3) adjusts the duty-cycle interval based on the percentage change between consecutive readings, ensuring high temporal resolution during flood events while conserving energy during quiescent periods. Expressing thresholds as a percentage of measured distance makes the algorithm self-normalizing across deployment heights. Post-hoc simulation against the field data showed that the 1%/3% configuration achieves 84% energy savings compared to the 1–2 minute test intervals while still resolving the river level rise dynamics.

Measurement uncertainty was assessed per ISO 4373:2022 [International Organization for Standardization 2022]: direct standard deviation for stable-river conditions, and de-trended residual analysis (moving-average subtraction, window=5) for changing-river conditions. Inter-sensor uncertainty was computed from 123 simultaneous co-located readings ($\sigma_{\text{diff}}/\sqrt{2}$).

3.1. Deployment Context

The sensor nodes communicate via LoRaWAN, a low-power wide-area protocol that achieves ranges up to 11 km in rural environments with an energy cost of 82.2 µWh per message [Orlovs et al. 2025]. The field deployments were conducted with infrastructure provided by the IoTec LAB, which has a project that comprises 20 gateways spanning 8 municipalities and serving a population of approximately 578,000 inhabitants in

the Foz do Rio Itajaí region. This existing infrastructure demonstrates the scalability of LoRaWAN-based monitoring for river basins. Figure 1 shows the bridge deployment site.

Figure 1. Lateral view of Bridge 2 from the river margin, showing the bridge structure and surrounding environment at the field deployment site.

4. Results

Water surface detection tests at 1–3 m over clear and turbid water revealed two key findings:

Table 3. Adaptive transmission strategy: duty-cycle intervals based on percentage change between consecutive readings [Ma et al. 2017].

Condition	Change Between Readings	Transmission Interval
Stable base-flow	$< 1\%$ of distance	15 minutes
Moderate activity	1–3% of distance	5 minutes
Rapid change	$> 3\%$ of distance	2 minutes

Turbidity improves LiDAR accuracy. Consistent with prior observations, turbid water improved LiDAR performance. The TF02-Pro error decreased from +7.2% (clear) to +2.0% (turbid) at 1 m, and its standard deviation at 3 m dropped from 50.0 mm to 22.2 mm. This is explained by Mie scattering from suspended particles enhancing surface reflectivity at near-infrared wavelengths [Bohren and Huffman 1998], consistent with the minimum turbidity threshold of $\sim$700 NTU reported in prior work [Jannata et al. 2021]. This finding is favorable for flood monitoring, since turbidity peaks precisely when accurate measurement is most critical.

TF-Nova beam interference. The TF-Nova's wide 14° line beam caused anomalous readings in confined environments, detecting tank edges at 3 m. During the rain

interference test, the wide beam detected the water spray curtain at 45 cm instead of the 500 cm target, while the TF02-Pro and JSN-SR04T were unaffected.

4.1. Field Deployment — Rainy Day

During the 5-hour overcast/rainy deployment (Feb 7), all three sensors tracked a 229 mm river level rise during a rainfall event (11 mm total precipitation), with consistent cross-sensor agreement (Figure 2).

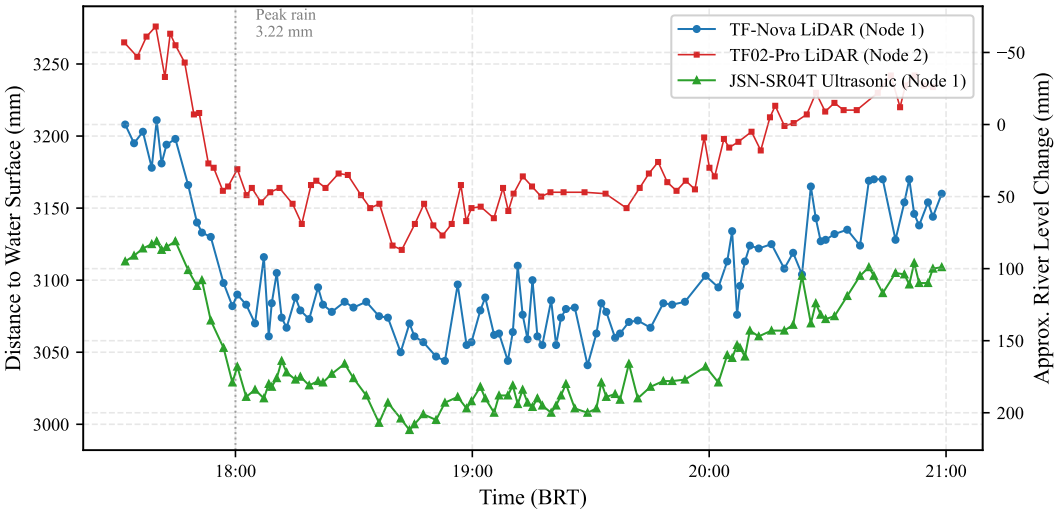

Figure 2. Sensor distance readings during rainy deployment (Feb 7, 2026). All sensors consistently track the 229 mm river level rise from 16:00 to 19:00 BRT.

Co-located TF-Nova and JSN-SR04T readings (123 simultaneous samples) showed a systematic offset of 54.9 mm (TF-Nova reading higher) with $\sigma_{\text{diff}} = 17.3$ mm, yielding a per-sensor uncertainty of $\sim$12.2 mm. All sensors achieved $\sim$95% valid reading rates under overcast conditions.

The DHT11 temperature sensor on the ultrasonic node failed during both deployments, causing the JSN-SR04T to use a fixed fallback temperature of 25°C for speed-of-sound compensation. A post-hoc correction using concurrent temperature readings from the second node (206 paired readings) showed mean corrections of 15 mm (0.50%) on the rainy day (28°C ambient) and 61 mm (1.86%) on the sunny day (36°C ambient). The sunny-day bias exceeds the ISO 4373 Class 3 threshold ($< \pm 1\%$), confirming that a functioning temperature sensor is essential for ultrasonic deployments in environments with significant thermal variation (Figure 3).

4.2. Field Deployment — Sunny Day

The clear-sky deployment (Feb 8) revealed the most significant finding of this study: ambient solar radiation as a dominant sensor-dependent failure mode (Table 4).

The TF-Nova experienced progressive degradation correlating with increasing solar irradiance: valid readings dropped from 69% in the morning to complete failure (0/50 readings) from 11:28 to 13:26 BRT. The TF02-Pro, operating on the same power rail, maintained 94.6% availability under identical conditions, ruling out power issues and

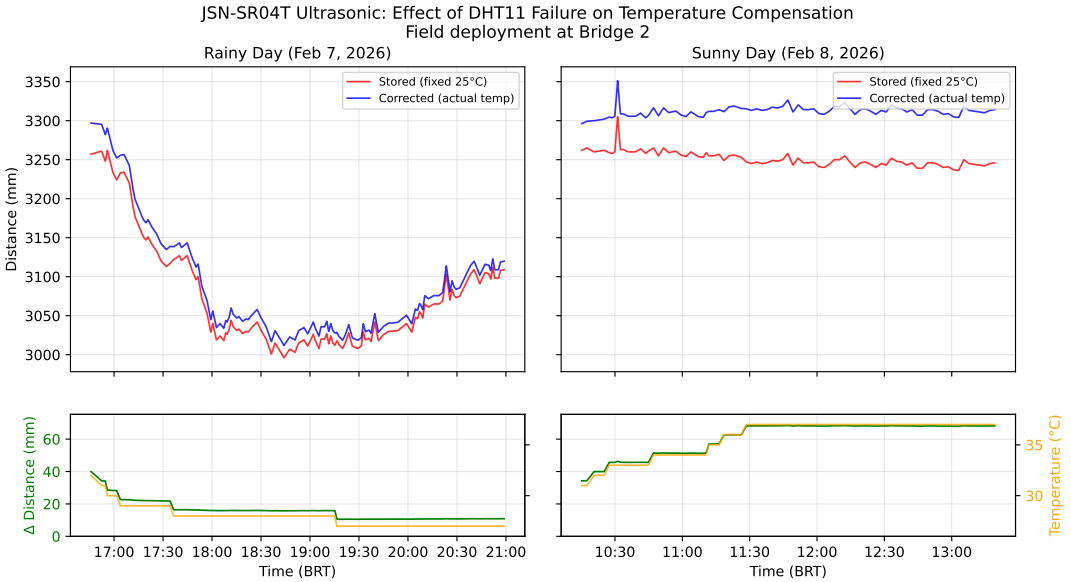

Figure 3. Effect of DHT11 failure on JSN-SR04T temperature compensation. Left: rainy day (28℃); right: sunny day (36℃). Upper panels: stored readings (red) vs. corrected (blue). Lower panels: correction magnitude (green) and ambient temperature (orange).

Table 4. Sensor performance during sunny deployment (Feb 8, 2026).

Sensor	Valid Rate	Mean (mm)	σ (mm)	Outliers
TF-Nova (LiDAR)	31.1%	3288.5	9.7	0
TF02-Pro (LiDAR)	94.6%	3355.1	67.5	4
JSN-SR04T (Ultrasonic)	94.4%	3251.3	9.8	2

confirming sunlight as the cause. The JSN-SR04T, operating in the acoustic domain, was completely immune.

This sensor-dependent vulnerability is explained by two design factors: the TF-Nova's 905 nm wavelength sits closer to the solar near-infrared peak than the TF02-Pro's 850 nm, and its wide 14° beam collects more ambient photons. The TF02-Pro was explicitly engineered for outdoor operation with 100 kLux ambient light immunity, while the TF-Nova has no sunlight rating. Water's low reflectivity and high solar intensity creates conditions where these differences become critical.

Figure 4 illustrates the dramatic contrast in TF-Nova behavior between overcast and sunny conditions.

4.3. Beam Geometry Effect

Bridge validation tests revealed a consistent advantage of the TF-Nova's line beam: up to 8$\times$ lower measurement variance than the TF02-Pro over water surfaces. The TF-Nova's 14° line beam illuminates an elongated footprint ($\sim$1.3 m at 5.4 m) that spatially averages wave peaks and troughs, acting as a low-pass filter. The TF02-Pro's 3° spot ($\sim$0.28 m footprint) captures instantaneous surface variations. Figure 5 shows the TF-Nova's wide aperture responsible for this effect.

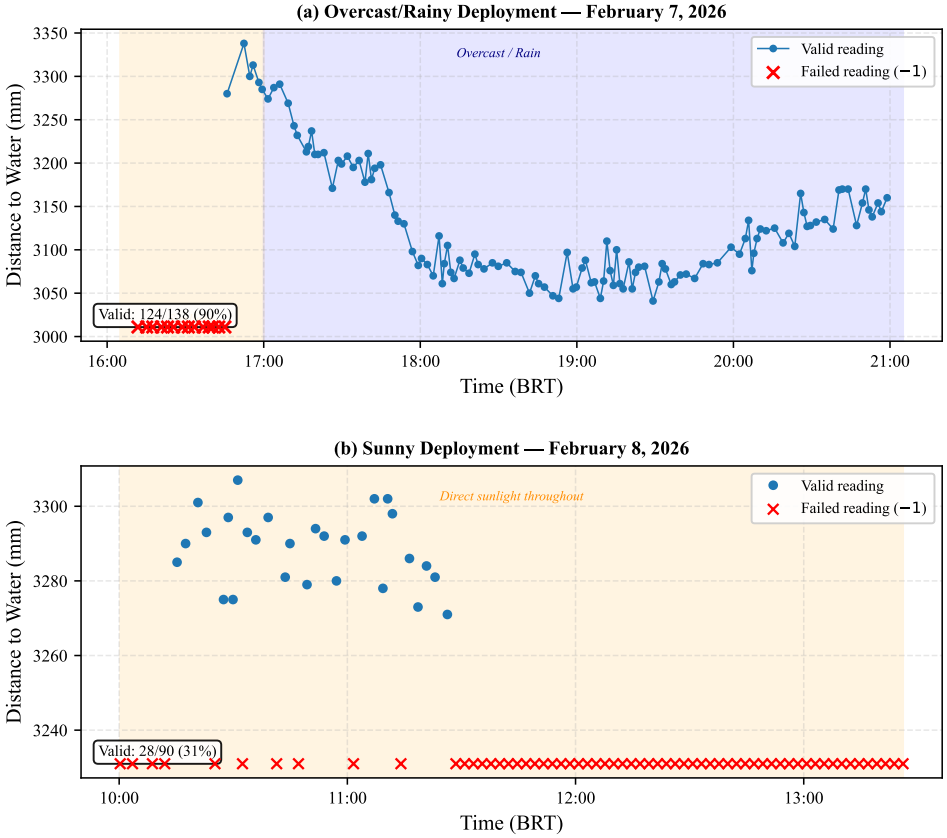

Figure 4. TF-Nova readings under overcast/rainy (Feb 7) versus sunny (Feb 8) conditions. Under overcast skies, readings are continuous and stable; under direct sunlight, availability drops to 31% with complete failure after 11:28 BRT.

This line-beam integration effect represents a trade-off: superior precision over open water but interference in confined environments (narrow channels, heavy rain curtains).

4.4. ISO 4373:2022 Compliance

Table 5 presents the ISO 4373:2022 performance classification results.

The JSN-SR04T is the only sensor achieving ISO 4373 compliance with reliable availability across all conditions. Its rainy-day uncertainty (6.8 mm, 0.22%) approaches Class 2, comparable to the ISO standard's reference performance for radar/laser sensors (5–10 mm). The TF02-Pro exceeded the Class 3 threshold due to spot-beam sensitivity to instantaneous water surface variations; multi-sample averaging would likely improve its classification. The TF-Nova achieved Class 3 precision ($\sigma = 9.7$ mm) when operational, but its 31% sunny-day availability limits practical deployment to shaded or overcast sites.

5. Discussion and Conclusion

This paper presented a comparative evaluation of three low-cost non-contact sensors for river level monitoring through controlled tests and field deployments under contrasting weather. The key contributions are: (1) identification of ambient solar radiation as a

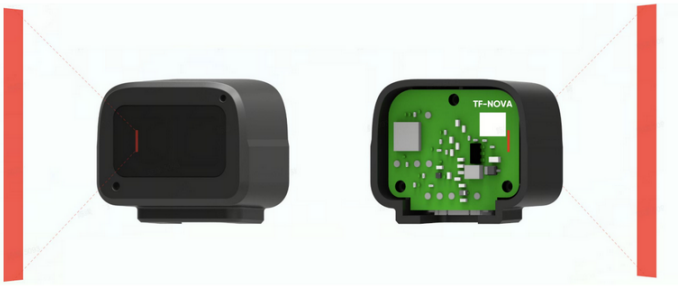

Figure 5. Optical aperture of the TF-Nova LiDAR. The wide emission window creates the 14° line-beam pattern responsible for the spatial averaging effect observed in field tests.

Table 5. ISO 4373:2022 performance classification (Class 1: <0.1%, Class 2: <0.3%, Class 3: <1.0%).

Sensor	Condition	σ (mm)	Uncert. (%)	Valid Rate	Class
JSN-SR04T	Sunny	9.8	0.30	94.4%	3
JSN-SR04T	Rainy	6.8	0.22	99.2%	$\sim$2
TF-Nova	Sunny	9.7	0.30	31.1%	3*
TF-Nova	Rainy	14.7	0.47	100%	3
TF02-Pro	Sunny	67.5	2.01	94.6%	>3
TF02-Pro	Rainy	51.6	1.58	100%	>3

*Class 3 precision achieved but limited by 31% availability.

critical, sensor-design-dependent LiDAR limitation (TF-Nova 31% vs. TF02-Pro 95% availability under identical sunny conditions); (2) characterization of beam geometry as a selection criterion, with the 14° line beam providing up to 8× stability improvement over spot beam; and (3) demonstration that water turbidity improves LiDAR accuracy [Jannata et al. 2021], favorable for flood monitoring where turbidity peaks when measurement is most critical.

These findings yield practical sensor selection guidelines. For bridges $\leq$4.5 m, the JSN-SR04T is recommended: IP67 protection, sunlight immunity, and ISO 4373 [International Organization for Standardization 2022] Class 3 compliance (approaching Class 2 under rain). For bridges >4.5 m with sun exposure, the TF02-Pro maintains 95% availability but needs multi-sample averaging for ISO compliance. For >4.5 m shaded sites, the TF-Nova offers superior precision via its line-beam integration effect.

Some limitations apply: $\sim$12 hours of field data across two deployments, tape measure reference ($\sim$20–30 mm uncertainty), and only two bridge sites. These do not affect relative sensor comparisons but constrain absolute accuracy assessment. Future work should include multi-month deployments with calibrated reference gauges, further testing of solar radiation and wind effects, and network-scale validation leveraging infrastructure such as the IoTec LAB regional LoRaWAN network.

Acknowledgments

This work was supported by the IoTec LAB, which provided the LoRaWAN infrastructure used in the field deployments. Large language models were used for reviewing the text of

this paper.

References

Bohren, C. F. and Huffman, D. R. (1998). *Absorption and Scattering of Light by Small Particles*. Wiley-VCH.

Borga, M., Stoffel, M., Marchi, L., Marra, F., and Jakob, M. (2014). Hydrogeomorphic response to extreme rainfall in headwater systems: Flash floods and debris flows. *Journal of Hydrology*, 518:194–205.

DAO, M.-H., ISHIBASHI, K., NGUYEN, T.-A., BUI, D.-H., HIRAYMA, H., TRAN, T.-A., and TRAN, X.-T. (2025). Low-cost, high accuracy, and long communication range energy-harvesting beat sensor with LoRa for water-level monitoring. *IEEE Sensors Journal*.

International Organization for Standardization (2022). Hydrometry — water-level measuring devices. International Standard ISO 4373:2022, ISO.

Jannata, M. S., Salam, R. A., and Suhendi, A. (2021). Study on the near-IR light detection and ranging (LiDAR) potential use as water level sensor. In *IOP Conference Series: Earth and Environmental Science*, volume 704, page 012040.

Jonkman, S. N. (2005). Global perspectives on loss of human life caused by floods. *Natural Hazards*, 34:151–175.

Kabi, J. N., Kamucha, G., and Maina, C. (2023). Low cost, LoRa based river water level data acquisition system. *HardwareX*.

Kupper, K. D., Sausen, J. P., and de Campos, M. (2025). Trends and technologies in environmental monitoring: A review of sensors, communication, and AI-enabled systems. In *2025 17th Seminar on Power Electronics and Control (SEPOC)*. IEEE.

Ma, Y., Liang, Y., Hsu, L., and Yeh, T.-H. (2017). An energy efficient adaptive sampling algorithm in a sensor network for automated water quality monitoring. *Sensors*, 17(11):2551.

MasoudiMoghaddam, M., Yazdi, J., and Shahsavandi, M. (2024). A low-cost ultrasonic sensor for online monitoring of water levels in rivers and channels. *Flow Measurement and Instrumentation*, 102:102777.

Mohammed, S., Al-Zubaidi, S., Ali, M., and Hussein, A. (2019). Highly accurate water level measurement system using a microcontroller and an ultrasonic sensor. *IEEE Sensors Journal*, 19(20):9107–9117.

Mohindru, P. (2023). Development of liquid level measurement technology: A review. *Flow Measurement and Instrumentation*, 89:102295.

Orlovs, D., Rusins, A., Skrastins, V., and Judvaitis, J. (2025). Comparative analysis of LPWAN technologies for environmental monitoring. *IoT*, 6(4).

Otto, F., Zachariah, M., Kew, S., Rodrigues, R., Philip, S., Pereira, P., Pinheiro, G., Singh, R., Arrighi, J., Vautard, R., van Aalst, M., and Alves, L. (2024). Climate change, El Niño and infrastructure failures behind massive floods in Rio Grande do Sul, Brazil. Technical report, World Weather Attribution.

Paul, J. D., Buytaert, W., and Sah, N. (2020). A technical evaluation of Lidar-based measurement of river water levels. *Water Resources Research*, 56.

Pereira, T. S. R., de Carvalho, T. P., Mendes, T. A., and Formiga, K. T. M. (2022). Evaluation of water level in flowing channels using ultrasonic sensors. *Sustainability*, 14:5512.

Pörtner, H.-O., Roberts, D. C., Tignor, M. M. B., Poloczanska, E. S., Mintenbeck, K., Alegría, A., Craig, M., Langsdorf, S., Löschke, S., Möller, V., Okem, A., and Rama, B. (2022). *Climate Change 2022: Impacts, Adaptation and Vulnerability*. Cambridge University Press.

Ragnoli, M., Leoni, A., Barile, G., Ferri, G., and Stornelli, V. (2020). An autonomous low-power LoRa-based flood-monitoring system. *IEEE Access*, 8:115934–115945.

Santos, C. F., Tornquist, C. S., and Marimon, M. P. (2014). Indústria das enchentes: Impasses e desafios dos desastres socioambientais no vale do itajaí. *DOAJ (Directory of Open Access Journals)*.

Sun, Z., Yang, H., Liu, K., Yin, Z., Li, Z., and Xu, W. (2022). Recent advances in LoRa: A comprehensive survey. *ACM Transactions on Sensor Networks*, 18.

Tamari, S. and Guerrero-Meza, V. (2016). Flash flood monitoring with an inclined Lidar installed at a river bank: Proof of concept. *Remote Sensing*, 8:834.

Tarulescu, R. and Tarulescu, S. (2014). The influence of wind speed and direction over the ultrasonic detection. In *Proceedings of SMAT 2014*.

Tawalbeh, R., Alasali, F., Ghanem, Z., Alghazzawi, M., Abu-Raideh, A., and Holderbaum, W. (2023). Innovative characterization and comparative analysis of water level sensors for enhanced early detection and warning of floods. *Journal of Low Power Electronics and Applications*, 13(2):26.

United Nations General Assembly (2015). Transforming our world: The 2030 agenda for sustainable development. Technical Report A/RES/70/1, United Nations.

United Nations Office for Disaster Risk Reduction (2015). Sendai framework for disaster risk reduction 2015–2030. Technical report, UNDRR.

Wu, Z., Huang, Y., Huang, K., Yan, K., and Chen, H. (2023). A review of non-contact water level measurement based on computer vision and radar technology. *Water*, 15:3233.